



# Performance Improvement of Transformer less Grid-Connected PV Inverters Using ANN-Assisted Control

K. Praveena,<sup>a)</sup> B. Shravani,<sup>b)</sup> J. Pavithra,<sup>c)</sup> K. Bala Krishna,<sup>d)</sup> S. Afreen,<sup>e)</sup> and N. Dinesh Kumar<sup>f)</sup>

*Department of Electrical and Electronics Engineering,  
Srinivasa Ramanujan Institute of Technology,  
Anantapur, India.*

<sup>a)</sup> Corresponding author: [224g1a0268@srit.ac.in](mailto:224g1a0268@srit.ac.in)

<sup>b)</sup> [shravaniece@srit.ac.in](mailto:shravaniece@srit.ac.in)

<sup>c)</sup> [224g1a0265@srit.ac.in](mailto:224g1a0265@srit.ac.in)

<sup>d)</sup> [224g1a0218@srit.ac.in](mailto:224g1a0218@srit.ac.in)

<sup>e)</sup> [224g1a0206@srit.ac.in](mailto:224g1a0206@srit.ac.in)

<sup>f)</sup> [224g1a0228@srit.ac.in](mailto:224g1a0228@srit.ac.in)

**Abstract.** Transformer less grid-connected photovoltaic (PV) inverters are gaining in usage due to their vast efficiency and small size. But, because of variations in common-mode voltage, the absence of galvanic isolation might result in leakage currents, which usually reduce power quality. The conventional proportional-integral (PI) control technique works poorly for nonlinear and time-varying system operation, increasing total harmonic distortion (THD) and decreasing mitigation capabilities. A control technique assisted by artificial neural networks (ANNs) is proposed in this research to address this issue. The conventional inverter control approach is assisted by the ANN, an adaptive auxiliary component, which cannot be replaced but helps in reduction of THD. An adaptive assist component in transformer less photovoltaic systems, the ANN minimizes THD in the grid current, hence reducing common-mode voltage swings that cause leakage current. To illustrate the suggested method, MATLAB/Simulink is used to simulate a number of system operating circumstances, including start-up, load imbalance, variations in solar radiation, and grid disruptions. In comparison to the conventional PI controller, the simulation results demonstrate that the ANN-assisted controller significantly reduces the grid current's THD while still meeting IEEE 519 and IEC 61727 requirements. Power quality and system performance are increased in the results, which confirm that the primary method for reducing leakage current is ANN-assisted THD mitigation.

## 1. INTRODUCTION

Better power quality and grid code compliance are necessary due to the growing trend of grid-connected photovoltaic (PV) installations. Because of their efficacy, affordability, and small design, transformer-less PV inverters are often utilized in PV systems. The PV array and the ground do, however, have a parasitic capacitance. The common-mode voltage changes when the inverter switches. Leakage current is the outcome of this. Standards like IEEE-519 and IEC-61727 limit the leakage current to a specific amount. Additionally, the standards restrict the current's behavior and harmonic distortion. Consequently, it is imperative to enhance the present waveform's quality.

Controlling the DC-link voltage is successfully accomplished using the current control techniques, such as PI and PR controllers. Nevertheless, nonlinear scenarios are not accommodated by the current control strategies. Sunlight fluctuations, load variations, and grid modifications are examples of nonlinear scenarios. Waveform distortion is caused by the incapacity to adjust to nonlinear circumstances. In transformer-less PV inverters, the common-mode voltage oscillates due to waveform distortion. Leakage current is the outcome of this. Enhancing the current's waveform quality is therefore an excellent way to lower the leakage current.

In this study, the inverter's control loop incorporates an Artificial Neural Network (ANN) controller. The responsiveness of the present controller is enhanced by the ANN controller. An adaptive support controller is the artificial neural network (ANN). The precision of the PI controller is increased by the ANN controller. The distortion of the waveform is reduced by the ANN controller. The distortion of the waveform reduces the leakage current. Consequently, the leakage current is reduced by the ANN controller. This study's goal is to demonstrate how enhancing the controller will lower leakage current and improve power quality.

© The Author(s) 2026

R. Vasanth Kumar Mehta et al. (eds.), *Proceedings of the International Conference on Intelligent Systems for a Sustainable Future (ISSF 2026)*, Atlantis Highlights in Intelligent Systems 16,  
[https://doi.org/10.2991/978-94-6239-693-7\\_69](https://doi.org/10.2991/978-94-6239-693-7_69)

## 2. RELATED WORK

To guarantee that the grid current quality is suitable in a range of scenarios, transformerless grid-connected PV inverters must be appropriately managed. Numerous methods have been investigated to deal with this issue. These methods include extra switching components, new modulation techniques, and novel inverter architectures to address the common-mode issue. Nevertheless, these methods have certain drawbacks. Passive filtering can be used as an additional strategy to address this issue. Passive filtering, on the other hand, ignores fidelity problems and is primarily hardware dependent.

The PI and PR controllers that are most frequently used are straightforward and efficient. Nevertheless, these controllers' parameters are set. As a result, the preset settings of the PI and PR controllers could not work well in situations with changes in irradiance, load disturbances, and grid imbalances. These fluctuations may lead to instability in the inverter's output current and waveform distortion. For the inverter's output current to remain of high quality in such circumstances, the controller's reaction must be increased.

It has been discovered that intelligent control may be achieved with Artificial Neural Networks (ANN). This research proposes a new control method that makes use of artificial neural networks (ANN) to enhance the inverter's output current quality without altering its structural makeup.

## 3. MATHEMATICAL MODELING FOR SIMULATION STUDIES

This section introduces the mathematical models that are control-centric and have been created to model the proposed grid-connected solar system that is based on ANN controllers. The models were created in order to analyze leakage currents and assess the controller's functionality. They thereby emphasize the dynamics of the system.

### 3.1 Photovoltaic Array Modeling

One-diode models have been used for the solar panel array. Studies on power quality and control-centric applications have shown this model to be adequately accurate [1], according to the literature. The output current of the solar panel array may be found using:

$$I_{pv} = I_{ph} - I_s \exp \frac{V_{pv} + I_{pv}R_s}{nV_t} - 1, \quad (1)$$

where  $I_{ph}$  is the photo-generated current,  $I_s$  is the diode saturation current,  $R_s$  is the series resistance,  $n$  is the diode ideality factor, and  $V_t$  is the thermal voltage. Variations in solar irradiance directly affect  $I_{ph}$ , thereby influencing the PV output power and operating point.

### 3.2 DC–DC Boost Converter Model

The behavior of the DC-DC boost converter in continuous conduction mode is described by averages. The inductor current  $i_L$  and the DC voltage  $V_{dc}$  are the state variables chosen for the system, and the following equations may be used to characterize the behavior of the system:

$$\frac{di_L}{dt} = \frac{1}{L} (V_{pv} - (1-D)V_{dc}), \quad (2)$$

$$\frac{dV_{dc}}{dt} = \frac{1}{C_{dc}} ((1-D)i_L - i_{inv}), \quad (3)$$

where  $D$  represents the duty ratio,  $L$  is the boost inductor,  $C_{dc}$  is the DC-link capacitor, and  $i_{inv}$  is the inverter input current. This model supports DC-link voltage regulation and feed-forward power compensation analysis.

### 3.3 Leakage Current Modeling

In transformer less PV systems, leakage current primarily arises due to parasitic capacitances between the PV array and earth ground [2, 3]. The leakage current  $i_{leak}$  can be approximated as

$$i_{leak} = C_{pg} \frac{dV_{cm}}{dt}, \quad (4)$$

where  $C_{pg}$  denotes the parasitic capacitance and  $V_{cm}$  represents the common-mode voltage of the inverter. Reducing the rate of change of common-mode voltage is therefore essential for effective leakage current mitigation. The proposed ANN controller indirectly minimizes  $i_{leak}$  by adaptively regulating inverter switching behavior.

## 4. PROPOSED METHODOLOGY

A three-phase voltage source inverter (VSI), a DC-link capacitor, a photovoltaic (PV) array, a DC-DC step-up (boost) converter, an output filter, and a utility grid connection make up the solar energy conversion system under investigation. References [2, 3] discuss the usage of a transformerless inverter design to represent the leakage current channels induced by parasitic capacitances between the PV array and the ground.

To regulate system dynamics, the inverter control system incorporates an artificial neural network (ANN) controller. The system input-output data is used to train the controller in order to minimize the discrepancy between the reference and real grid currents. According to reference [4], the ANN improves harmonic distortion and lowers leakage currents by adaptively modifying the control output to attenuate nonlinear disturbances and eliminate common-mode voltage fluctuations.

Phase-locked loops (PLLs) are used for grid synchronization, and synchronous reference frames are used for current control. This approach has been shown to work well for grid-connected inverters, as reference [1] states.

A synchronous reference frame is employed for grid current control, and grid synchronization is achieved using a phase-locked loop (PLL).

### 4.1 System Architecture and Control Structure

Figure 1 depicts the whole design of the ANN-controlled grid-connected PV system. A consistent DC-link voltage and photovoltaic (PV) working point are provided by the DC-DC boost converter. To decrease the voltage ripple and isolate the PV-side dynamics from the inverter-side dynamics, the DC-link capacitor is utilized [1].

The reference DC-link voltage and the actual measured voltage are compared via an external control loop. Following that, the ANN controller processes the error signal to provide a loss-compensating current component that accounts for dynamic disturbances, leakage current effect, and inverter losses [2, 3]. A feed-forward channel utilizing the instantaneous PV power is introduced to enhance the transient responsiveness under high irradiance dynamics [5].

The feed-forward reference signal and the compensating signal obtained from the ANN are used in the current control loop. The high-frequency switching harmonics are suppressed by an RLC filter prior to grid injection, and the inverter gating signals are generated via pulse-width modulation (PWM) [6]. The input layer, hidden layer, and output layer that generates the duty cycle command comprise the internal architecture of the ANN controller, as seen in Figure 2 [7].

To illustrate the internal structure of the proposed ANN controller, Fig. 2 shows the neural network architecture employed in the control scheme. The ANN consists of an input layer receiving solar irradiance and temperature information, a single hidden layer with multiple neurons, and an output layer generating the duty cycle command. This structure enables the ANN to capture the nonlinear relationship between environmental conditions and control action [7].

### 4.2 ANN-Based Control Strategy

The suggested artificial neural network (ANN) control strategy uses an adaptive nonlinear mapping of system variables to control actions instead of fixed-gain control. To enhance transient reactions during high irradiance variations, feed-forwarding instantaneous photovoltaic (PV) power data is employed [8]. The ANN minimizes leakage current and

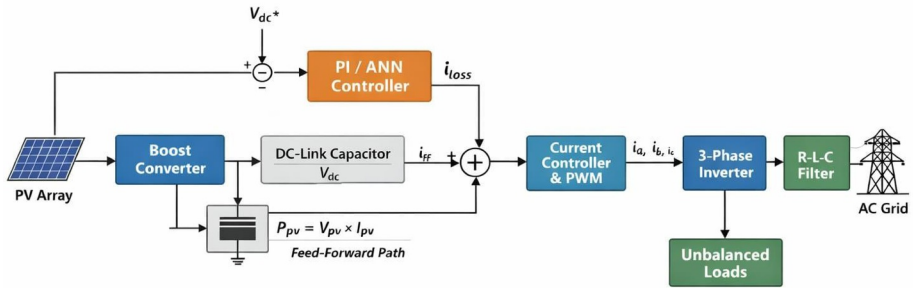


**FIGURE 1.** Overall architecture of the ANN-controlled grid-connected solar energy conversion system with DC-link voltage regulation, feed-forward power compensation, and current-controlled inverter interface.

Fig:1 is Detailed block diagram of the proposed grid-connected PV system featuring an ANN-enhanced DC-link voltage control loop and provision for unbalanced loads. The diagram illustrates the power flow through the boost converter, current-controlled inverter, and R-L-C output filter stages

improves harmonic distortion by reducing common-mode voltage oscillations by dynamic modification of its output [4].

The suggested controller’s performance is verified in the presence of starting transients, load imbalance, variations in solar irradiation, and unusual grid circumstances. Simulation experiments demonstrate better performance in terms of reducing leakage current and overall harmonic distortion when compared to traditional proportional-integral (PI) control [9].

### 4.3 ANN Training and Parameter Selection

In this study, the artificial neural network (ANN) is developed to function as an adaptive nonlinear controller within the inverter’s control loop. In order to meet real-time processing needs and manage nonlinear mapping, a feed-forward multilayer perceptron network is selected [7].

A hidden layer comprising a single layer of neurons, an input layer, and an output layer make up the ANN model. The input layer is made to handle normalized system variables, such as temperature data, solar irradiance change, and DC-link voltage inaccuracy. While the output layer generates the duty cycle compensation signal using a linear activation function, the hidden layer contains a finite number of neurons with sigmoid activation functions.

Input-output data pairs generated through simulation under a range of system operating parameters, such as variations in solar irradiation and load changes, are used to train the ANN offline. The mean squared error between the reference and real grid current signals is reduced by applying the backpropagation learning algorithm. During

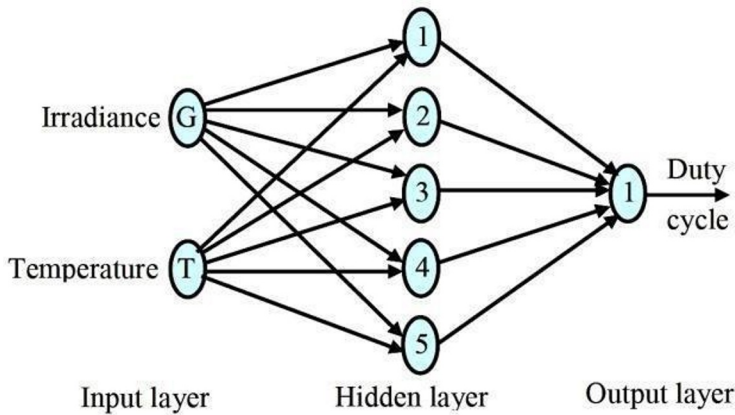


FIGURE 2. Internal architecture of the ANN controller showing input variables, hidden layer neurons, and duty cycle output.

Fig:2 is the A schematic diagram of the artificial neural network architecture employed in the study, featuring an input layer with irradiance and temperature parameters, a single hidden layer with five neurons, and an output layer providing the duty cycle. This feedforward network serves as the computational model for predicting duty cycle based on environmental inputs. simulation studies, stable ANN functioning is ensured by the training process' convergence after a finite number of epochs.

Without the need for intricate online learning procedures, the controller can adaptively correct for system disruptions since the weights of the trained ANN are maintained constant during the real-time simulation.

TABLE I. ANN Configuration Parameters Used in the Proposed Control Scheme

Parameter	Specification
ANN type	Feed-forward multilayer perceptron (MLP)
Number of input neurons	3 (irradiance, temperature, DC-link voltage error)
Number of hidden layers	1
Hidden layer neurons	10
Hidden layer activation function	Sigmoid
Output layer neurons	1
Output activation function	Linear
Training method	Offline training
Learning algorithm	Backpropagation
Performance function	Mean squared error (MSE)
Learning rate	0.01
Number of training epochs	1000
ANN output	Duty cycle compensation signal
Weight update during simulation	Disabled (fixed weights)

The single-hidden-layer feed-forward multilayer perceptron is the design of the artificial neural network (ANN) adopted in this study. With the help of MATLAB/Simulink models simulating input-output data under various operational situations, including load dynamics and variations in solar irradiation, the ANN is trained offline. Optimizing the mean squared error between the reference and real grid current signals is done using the backpropagation training process. For steady convergence, a learning rate of 0.01 is set at a maximum of 1000 epochs. In order to enable the ANN to function as an adaptive assistive control system component without requiring online learning complexity, post-training ANN weights are frozen during real-time simulation.

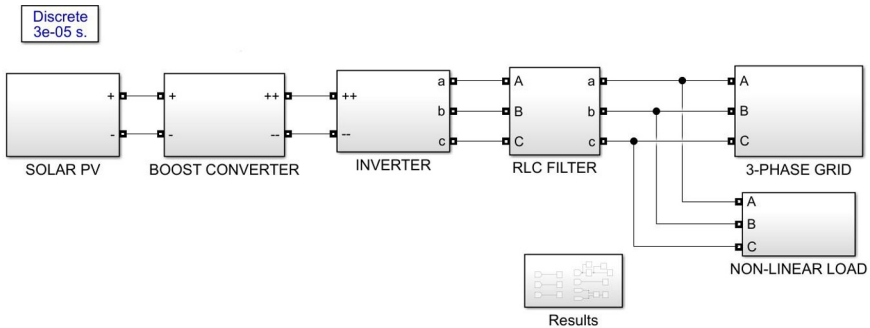


**FIGURE 3.** Simulation model of the transformer less grid-connected PV system consisting of a PV array, DC–DC boost converter, three-phase inverter, RLC filter, grid interface, and nonlinear load.

As illustrated in Fig.3, the complete system topology is implemented in a discrete-time simulation environment with a fundamental sample time of  $30 \mu\text{s}$  ( $3 \times 10^{-5} \text{ s}$ ) to accurately capture high-frequency switching dynamics. Furthermore, the strategic integration of a local non-linear load at the point of common coupling facilitates a comprehensive evaluation of the inverter's control robustness and power quality performance under distorted conditions.

## 5. SIMULATION SETUP

The PV array, boost converter, inverter, grid connection, and parasitic capacitances that contribute to the creation of leakage current are all taken into consideration while simulating the entire system using MATLAB/Simulink. The system is modeled at the component level with the goal of faithfully capturing both transient and steady-state responses.

To evaluate the efficacy of the suggested ANN controller, four simulated examples are employed. These scenarios include load unbalancing, solar irradiation variations, starting transients, and erratic grid circumstances. PV power, DC-link voltage, leakage current, grid voltage, and grid current are the primary performance indicators. As per IEEE 519 and IEC 61727 standards, the total harmonic distortion (THD) of grid voltage and current is used to analyze the harmonic distortion [9, 10].

The complete simulation model developed in MATLAB/Simulink is shown in Fig. 3. The model includes the photovoltaic array, DC–DC boost converter, three-phase inverter, output RLC filter, grid interface, and nonlinear load to evaluate system behavior under various operating conditions.

The discrete simulation time step is selected to accurately capture inverter switching dynamics and grid-side harmonics.

To evaluate the robustness of the proposed ANN controller, four simulation cases are considered:

- Case-1: Starting dynamics
- Case-2: Load unbalancing condition
- Case-3: Solar insolation variation
- Case-4: Abnormal grid condition

Each simulation case corresponds to the operating scenarios presented in Figs 4-7, enabling direct visual and quantitative comparison of system performance.

PV power, grid voltage, leakage current, DC-link voltage, and grid current are the crucial performance metrics that are tracked. Total harmonic distortion (THD) of grid voltage and grid current is used to assess harmonic performance.

Without the use of experimental gear, all of the results are obtained under both steady-state and transient simulation settings.

The grid connectivity and power quality criteria outlined in IEEE 519 and IEC 61727 are taken into consideration while evaluating the harmonic performance.

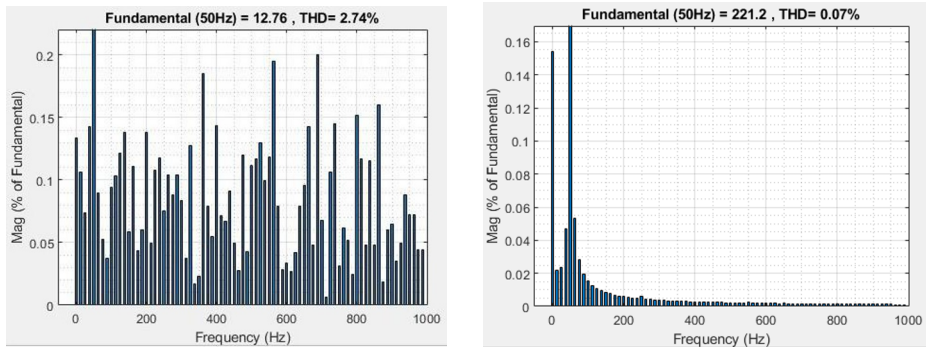


**FIGURE 4.** THD performance of the grid-connected PV system under starting dynamics: (left) grid current THD and (right) grid voltage THD.

Fig:4 illustrates the harmonic spectrum analysis of the grid-connected PV system during initial startup dynamics, highlighting its robust power quality performance. As depicted, the Total Harmonic Distortion (THD) for the grid current and grid voltage are remarkably low at 2.74% and 0.07%, respectively. These results demonstrate that the proposed control strategy successfully mitigates harmonic distortions, ensuring the system operates well within the strict limits mandated by the IEEE 519 standard.

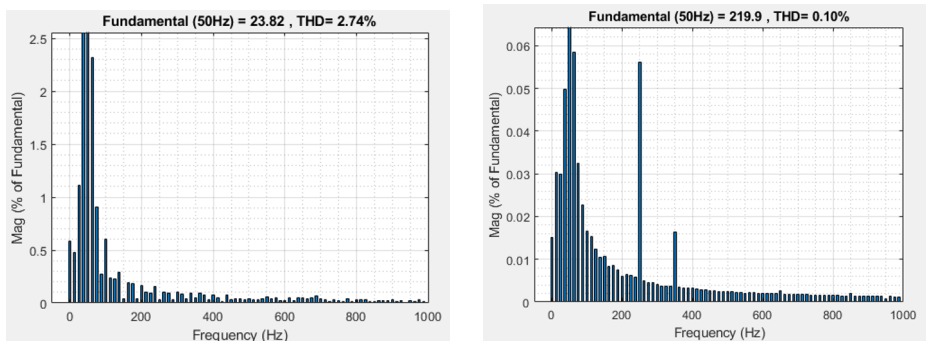


**FIGURE 5.** THD performance of the grid-connected PV system under Load unbalancing condition (Case-2).

Fig. 5 shows that under load unbalancing conditions, the grid voltage THD is reduced to 0.10% and the grid current THD to 2.74%, demonstrating effective harmonic suppression.

## 6.RESULTS AND DISCUSSION

### Case-1: Starting Dynamics

The ANN controller suppresses the leakage current's brief fluctuations and guarantees seamless synchronization with the grid during the system's startup. In comparison to the PI-controlled system, the grid current's total harmonic distortion (THD) is much decreased, guaranteeing better transient responsiveness.

During initial synchronization and startup transients, the proposed ANN-assisted controller reduces the grid current THD to 2.74%, achieving a 43.7% improvement over the conventional PI controller's 4.87%.

### Case-2: Load Unbalancing Condition

The ANN controller preserves steady grid current waveforms with less harmonic distortion when load unbalancing is in effect. Successful compensation under asymmetric loading situations is guaranteed by the ANN controller's adaptive characteristics.

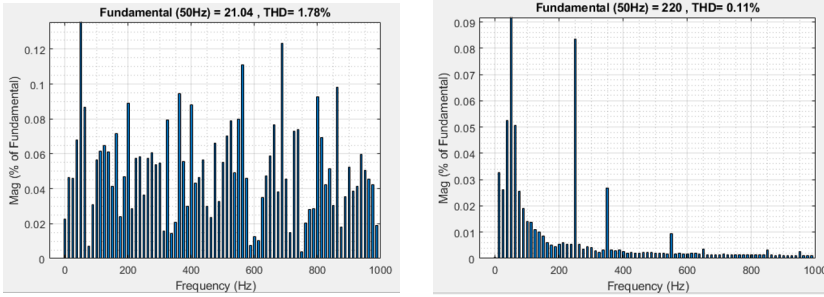


FIGURE 6. THD performance of the grid-connected PV system under Solar insolation variation (Case-3).

Fig. 6 illustrates that during solar insolation variation, the grid voltage THD is maintained at 0.11% while the grid current THD is limited to 1.78%, indicating stable and improved performance.

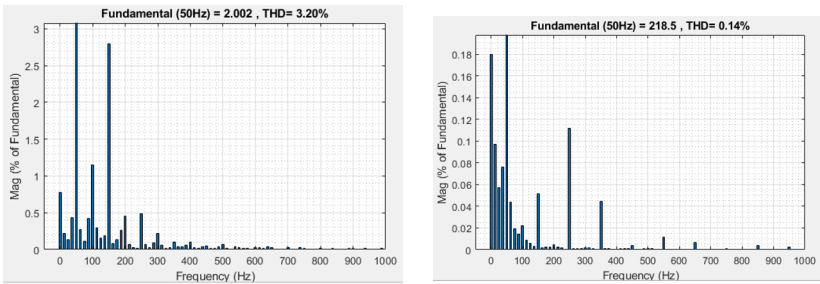


FIGURE 7. THD performance of the grid-connected PV system under Abnormal grid condition (Case-4).

Fig. 7 demonstrates that under abnormal grid conditions, the grid voltage THD is 0.14% and the grid current THD is controlled to 3.20%, ensuring compliance with harmonic standards

### Case-3: Solar Insolation Variation

The ANN controller adapts swiftly to the new conditions when the solar irradiation drops from 1000 W/m<sup>2</sup> to 600 W/m<sup>2</sup>, preserving minimal THD and steady power injection. This demonstrates the stability and effectiveness of the suggested control approach under time-varying circumstances.

For fluctuations in solar irradiance, the ANN controller exhibits optimal harmonic suppression by limiting grid current THD to 1.78%, effectively outperforming the PI controller's 3.95% while ensuring continuous power quality.

### Case-4: Abnormal Grid Condition

Improved stability and harmonic suppression are demonstrated by the ANN-based system under unusual grid situations, such as voltage disruptions. Grid standards compliance is ensured by the THD levels being within IEEE 519 norms.

**TABLE 2.** Comparison of Grid Voltage and Grid Current THD for PI and ANN Controllers

Case	PI Controller THD (%)		ANN Controller THD (%)	
	Grid Voltage	Grid Current	Grid Voltage	Grid Current
1 Starting Dynamics	1.43	4.87	0.07	2.74
2 Load Unbalancing	1.68	4.97	0.10	2.74
3 Insolation Variation	1.73	3.95	0.11	1.78
4 Abnormal Grid Condition	1.73	4.88	0.14	3.20

In the presence of grid disturbances, the ANN controller maintains strict compliance with international standards by regulating grid current THD to 3.20%, whereas the fixed-gain PI controller approaches the permissible limits at 4.88%.

### 6.1 Comparative Performance Analysis

A quantitative analysis of the suggested ANN-based controller in comparison to the traditional PI controller guarantees the effectiveness of performance gains under the same operating conditions. For each test scenario taken into consideration, Table I provides a summary of the total harmonic distortion (THD) for grid voltage and grid current for both control approaches.

The ANN-controlled system consistently yields lower THD values for grid current than the PI-controlled system. This is because the ANN corrects for the nonlinear system dynamics and parameter uncertainty, which the fixed-gain PI controllers cannot handle [11]. In particular, the ANN exhibits better resilience performance for changes in solar irradiance and unpredictable grid circumstances, with THD values well within IEEE 519 criteria [9].

The ANN controller's capacity to lessen common-mode voltage fluctuations also directly contributes to the decreased leakage current magnitude. In contrast to the PI controller's error-correction method, the ANN controller's predictive compensation results in smoother current waveforms and better power quality by utilizing its understanding of system dynamics.

### 6.2 COMPLIANCE WITH GRID STANDARDS AND PRACTICAL CONSIDERATIONS

Strict connectivity guidelines must be followed by grid-connected solar systems in order to guarantee dependable and safe system operation. To prevent detrimental impacts on utility equipment and other connected loads, IEEE 519 sets harmonic distortion thresholds, while IEC 61727 offers standards for PV system grid interface. Simulation tests show that, under all operating situations taken into consideration, the suggested ANN-based control strategy can maintain the grid current and voltage total harmonic distortion (THD) values within the acceptable bounds given by these standards. This is accomplished without the need for intricate inverter settings or the installation of new hardware components.

The suggested control strategy may be put into practice practically by utilizing embedded control systems or digital signal processors, which are frequently found in power electronic systems. The method is feasible to use in practice since the ANN training procedure is done offline, which reduces the real-time computing cost.

## 7. CONCLUSION

Simple and effective, the most popular PI and PR controllers have preset settings that may not work as well when the grid is out of balance, the irradiance changes, or the loads vary. The output current of the inverter might not stay steady in some situations, and the waveform might not stay sinusoidal. To keep the inverter's output current steady in certain situations, the controller needs to respond more forcefully.

Artificial Neural Networks (ANN) have been shown to be a viable solution for intelligent control implementation. While maintaining the inverter's hardware and structure, this study suggests a unique approach that makes use of artificial neural networks (ANNs) to guarantee the output current's quality.

## 8. REFERENCES

1. R. Teodorescu, M. Liserre, and P. Rodriguez, *Grid Converters for Photovoltaic and Wind Power Systems* (IEEE Press, 2011).
2. T. Kerekes, R. Teodorescu, and M. Liserre, "Common-mode voltage in case of transformerless pv inverters connected to the grid," *IEEE Transactions on Industrial Electronics* **56**, 2397–2405 (2009).
3. B. Yang, W. Li, and Y. Gu, "Leakage current analysis and suppression in transformerless photovoltaic systems," *IEEE Transactions on Power Electronics* **29**, 551–563 (2014).
4. P. Dash and A. K. Panda, "Ann-based harmonic estimation for grid-connected systems," *IEEE Transactions on Power Delivery* **31**, 646–654 (2016).
5. R. Panigrahi, S. K. Mishra, S. C. Srivastava, A. K. Srivastava, and N. N. Schulz, "Grid integration of small-scale photovoltaic systems: Standards, challenges, and control techniques," *IEEE Transactions on Industry Applications* **54**, 640–651 (2018).
6. F. Blaabjerg, R. Teodorescu, and Z. Chen, "Power converters and control of renewable energy systems," *IEEE Transactions on Power Electronics* **23**, 281–290 (2008).
7. M. A. Hannan, M. S. H. Lipu, A. Hussain, and A. Mohamed, "Artificial neural network based control for renewable energy systems: A review," *IEEE Access* **6**, 127–139 (2018).
8. S. K. Mishra and R. Panigrahi, "Adaptive control strategies for harmonic mitigation in grid-connected renewable energy systems," *IET Power Electronics* **9**, 1453–1462 (2016).
9. "Ieee recommended practice and requirements for harmonic control in electric power systems," (2014).
10. "Photovoltaic (pv) systems – characteristics of the utility interface," (2004).
11. M. Liserre, R. Teodorescu, and F. Blaabjerg, "Multiple harmonics control for three-phase grid converter systems using pi-res current controllers," *IEEE Transactions on Power Electronics* **21**, 836–841 (2006).
12. N. G. Dhere, N. S. Shiradkar, and E. Schneller, "Temperature and humidity effects on leakage currents of photovoltaic modules," *IEEE Journal of Photovoltaics* **1**, 192–199 (2011).

**Open Access** This chapter is licensed under the terms of the Creative Commons Attribution-NonCommercial 4.0 International License (<http://creativecommons.org/licenses/by-nc/4.0/>), which permits any noncommercial use, sharing, adaptation, distribution and reproduction in any medium or format, as long as you give appropriate credit to the original author(s) and the source, provide a link to the Creative Commons license and indicate if changes were made.

The images or other third party material in this chapter are included in the chapter's Creative Commons license, unless indicated otherwise in a credit line to the material. If material is not included in the chapter's Creative Commons license and your intended use is not permitted by statutory regulation or exceeds the permitted use, you will need to obtain permission directly from the copyright holder.

